Mathematical Geology, Vol. 13, No. 5, 1981

Application of the Buffon Needle Problem and its Extensions to Parallel-Line Search Sampling Scheme[1]

C. F. Chung[2]

Buffon's needle problem is generalized to a grid of unequally spaced parallel strips and a needle with a preferred orientation. This generalization is useful to determine the spacing of flight lines for locating anomalies by airborne geophysical surveys.

KEY WORDS: Buffon needle problem, geometric probability, geophysical surveys, unequally spaced parallel strips, preferred orientation.

INTRODUCTION

A common strategy for locating hidden anomalies by airborne geophysical surveying consists of searching along regularly spaced flight lines. Problems with aircraft navigation cause these lines to appear as approximately parallel traverse lines on maps as shown in Fig. 1. An anomaly is considered to be located if any of the traverse lines intersect it. Buffon's problem and its solutions have been applied to calculate the probability of intersection for a given spacing and to determine the spacing of flight lines for a given probability level by Agos, 1955 and McCammon, 1977.

However, there are the following several difficulties in applying Buffon's problem to certain types of geophysical surveys, such as airborne radiometric surveys (Grasty, Kosanke, and Foote, 1979)

1. surveys are performed along lines but respond to strips of ground;
2. lines are not equally spaced as in Fig. 1;
3. lines are not parallel to each other; and
4. sometimes, the anomalies have a preferred orientation.

---

[1]Manuscript received 5 December 1980; revised 31 March 1981. Paper presented at Session on Geometrical Probability and Statistical Problems in the Geosciences, American Statistical Association Annual Meeting, Houston, Texas, August 11–14, 1980.

[2]Geological Survey of Canada, 601 Booth Street, Ottawa, Canada K1A 0E8.

0020-5958/81/1000-0371$0.300/0

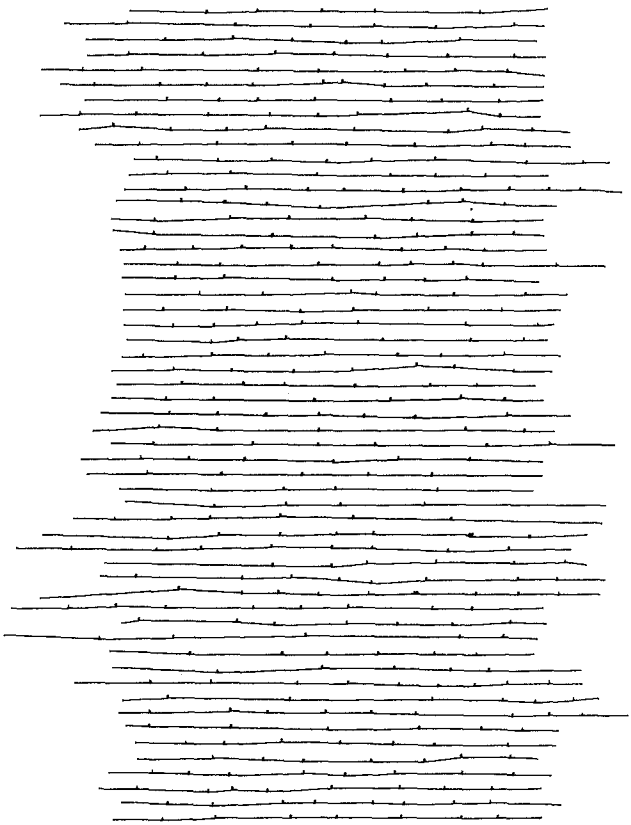

Fig. 1. Flight path map for a survey flown in the Sharbot Lake Area of Eastern Ontario to investigate occurrences of uranium mineralization. The spacings between flight paths are, approximately, between 375 and 625 m.

In this paper, the problem is generalized to cover points 1, 2, and 4. It should also be noted that geophysical anomalies, in reality, have considerably more complex geometrical shapes than the simple line segment considered. In addition, statement 1 above is a simplified approximation to actual coverage by airborne surveys (Grasty, Kosanke, and Foote, 1979).

Buffon's problem and several of its variations are described followed by a generalization of the problem. The results are then applied to a practical example.

BUFFON NEEDLE PROBLEM AND ITS VARIATIONS

Buffon's problem considers a grid of parallel lines with spacing d and a needle T of length l as shown in Fig. 2. When the needle T is dropped "at ran-

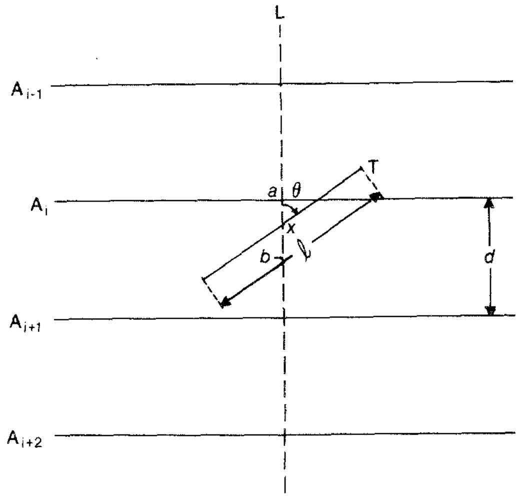

Fig. 2. Buffon's problem. A_is are a part of a grid of parallel lines with equispacing d. The line L is perpendicular to the parallel lines in the grid and passes through the midpoint x of the needle T of length l. θ is the angle from L to T, a is the crossing point of L and A_i and b is the midpoint on L between two parallel lines A_i and A_{i+1}. Without loss of generality it can be assumed that x is uniformly distributed in the interval $[a, b]$ and θ takes a value in $[-\pi/2, \pi/2]$, when T is dropped "at random" on the grid. The probability that T intersects at least one of the parallel lines is given in eq. (1).

dom" so that its position and orientation are random, the probability p_b that T intersects at least one line of the grid is given by

$$p_b = \begin{cases} \dfrac{2l}{\pi d}, & l \leqslant d \\ \dfrac{2l}{\pi d} + \dfrac{2a_0}{\pi} - \dfrac{2l}{\pi d} \sin a_0, & l > d \end{cases} \tag{1}$$

where $a_0 = \cos^{-1}(d/l)$. Proofs are given, among many others, by Kendall and Moran (1963) and Solomon (1978). Let us now consider the following three variations of this problem.

Parallel Strips

Instead of taking a grid of parallel lines, let us consider a grid of parallel strips shown in Fig. 3. A strip of breadth w is defined by the closed part of the

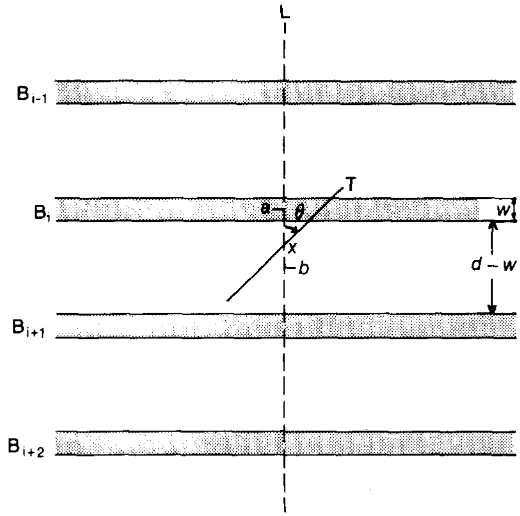

Fig. 3. x, θ, T, and L are same as in Fig. 2. B_is are a part of a grid of parallel strips of breadth w with equispacing $d - w$. a is the midpoint on L in B_i and b is the midpoint on L between B_i and B_{i+1}. When T is dropped at random we may assume that $x \in [a, b]$ and $\theta \in [-\pi/2, \pi/2]$ and the probability that T intersects at least one of the strips is given in eqs. (2) and (3) depending upon l.

plane consisting of all points that lie between two parallel lines at distance w from each other (Santalo, 1976). The position and orientation of a strip are determined by its center line. Suppose that the spacing between two adjacent strips is $d - w$; then the probability p_s of the intersection is given by Santalo (1976)

$$p_s = \frac{2l}{\pi d} + \frac{w}{d}, \qquad l \leqslant d - w \tag{2}$$

For a longer needle with $l > d - w$, the probability p_s is obtained from

$$p_s = \frac{4}{\pi d} \int_0^{a_0} \int_0^{d/2} dx\, d\theta + \frac{4}{\pi d} \int_{a_0}^{\pi/2} \int_0^{x_0} dx\, d\theta$$

$$= \frac{2l}{\pi d} + \frac{w}{d} + \frac{2a_0}{\pi} - \frac{2l}{\pi d} \sin a_0 - \frac{2wa_0}{\pi d} \tag{3}$$

where $a_0 = \cos^{-1} \{(d - w)/l\}$ and $x_0 = (w + l \cos \theta)/2$. Equations (2) and (3) are extensions of eq. (1) and $p_s = p_b$ if $w = 0$.

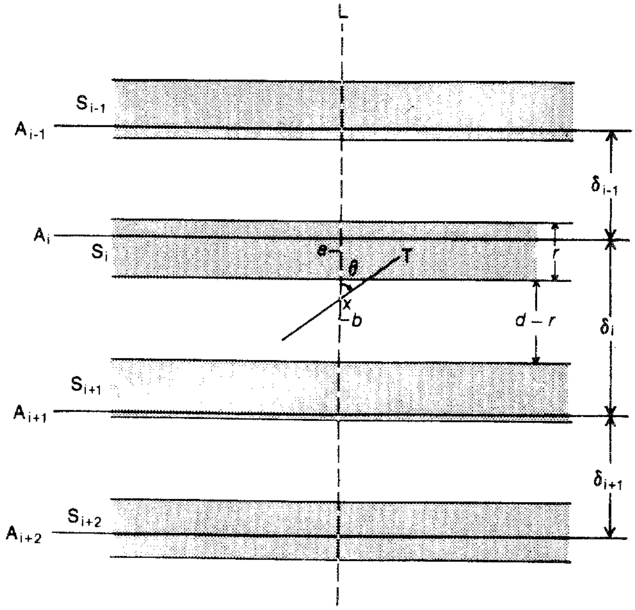

Fig. 4. x, θ, T, and L are the same as in Fig. 2. A grid of parallel lines A_is are formed by selecting one random line A_i from each strip S_i where S_is are a part of a grid of strips with breadth r and equispacing $d - r$. Of course, the spacings δ_is are not identical to each other. a is the midpoint on L within S_i and b is the midpoint between S_i and S_{i+1} on L. When T is dropped at random on the grid eq. (4) gives the probability of intersection.

Unequally Spaced Parallel Lines

Let us consider a grid of parallel lines formed by taking a parallel line at random within each of the parallel strips as shown in Fig. 4. Obviously, the spacings between adjacent pairs of parallel lines of this grid are not identical as is the case in Buffon's problem. Suppose that $r \leqslant d/2$ for simplicity. Then, for $l \leqslant d - r$, the probability p_u of intersection is obtained from

$$p_u = \frac{4}{\pi d} \int_0^{a_1} \left[\int_0^{x_1} dx + \int_{x_1}^{x_2} \frac{x_2 - x}{r} dx \right] d\theta$$

$$+ \frac{4}{\pi d} \int_{a_1}^{\pi/2} \left[\int_0^{x_3} \frac{l \cos \theta}{r} dx + \int_{x_3}^{x_2} \frac{x_2 - x}{r} dx \right] d\theta$$

$$= \frac{2l}{\pi d} \tag{4}$$

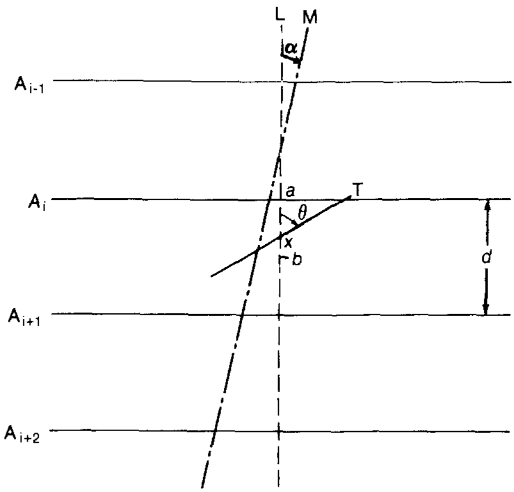

Fig. 5. x, θ, T, L, a, b, and A_is are the same as in Fig. 2. T is dropped on the grid such that θ has the density function in eq. (6). The line M shows the preferred orientation α of T, and the probability of intersection is given in eq. (7).

where

$$x_1 = \tfrac{1}{2} r - \tfrac{1}{2} l \cos\theta,$$

$$x_2 = \tfrac{1}{2} r + \tfrac{1}{2} l \cos\theta,$$

$$x_3 = -\tfrac{1}{2} r + \tfrac{1}{2} l \cos\theta, \text{ and}$$

$$a_1 = \begin{cases} \cos^{-1}\left(\dfrac{r}{l}\right), & l > r \\ 0, & l \leqslant r \end{cases}$$

However, when the expectation $E(s)$ of the spacing s is known, p_u can also be obtained from (Watson, 1978);

$$p_u = \frac{2l}{\pi E(s)} \tag{5}$$

Of course, $E(s) = d$ in this situation, because the spacing s has a symmetric triangular density function with the apex at $s = d$. Hence p_u in eq. (5) is identical to that of eq. (4).

Needle with a Preferred Orientation

Suppose that the orientation of the needle is distributed about "a preferred orientation α" shown in Fig. 5, instead of the uniformly distributed orientation as has been assumed in Buffon's problem. The most commonly used distribution to describe preferred oriented angles is the Von Mises distribution which is sometimes referred to as "circular normal" (Johnson and Kotz, 1970). However, Marriot (1969) has proposed the following density function to describe such preferred oriented angles

$$f(\theta) = \frac{1}{\pi}(1 + K \cos 2(\theta - \alpha)), \qquad -\frac{\pi}{2} \leqslant \theta \leqslant \frac{\pi}{2}, \qquad -1 \leqslant K \leqslant 1 \tag{6}$$

This density function is much simpler to handle than the Von Mises distribution and Marriot (1969) has studied its properties and the maximum likelihood estimation of α and K, where α and K are the location and scale parameters, respectively. Subsequently, Marriot (1971) has shown that, for a preferred orientation α of the needle of length $l \leqslant d$, the probability p_p of the intersection is given by

$$p_p = \frac{2l}{\pi d} + \frac{2lK}{3\pi d} \cos 2\alpha, \qquad l \leqslant d, \qquad 0 \leqslant \alpha \leqslant \frac{\pi}{2}, \qquad -1 \leqslant K \leqslant 1 \tag{7}$$

These results can be extended to a longer needle of $l > d$. However, that will be discussed as a special case in the next section.

UNEQUALLY SPACED PARALLEL STRIPS AND A NEEDLE WITH A PREFERRED ORIENTATION

In this section, not only the combination of all three previous variations, but also the cases without restriction on the length of the needle T, are described. Let us consider a grid of parallel strips of breadth r with spacing $d - r$. A grid of parallel strips of breadth w is constructed by taking a strip of breadth w at random within each parallel strip of breadth r, as shown in Fig. 6. Of course, the spacings between adjacent strips of breadth w are not identical. Suppose that a needle T of length l is dropped on the grid and the direction θ has a preferred orientation α with the density function in eq. (6).

To simplify the calculation of the probability that T intersects at least one of the strips, the restriction, $w \leqslant \frac{1}{2}r \leqslant \frac{1}{4}d$ is imposed on the parameters of the grid. Without the restriction, the probability has a complex analytic form. However, most real situations satisfy the restriction which indicates that the breadth w of A_is is less than the half of r of S_is and r is less than the half of d in Fig. 6.

With the restriction, the probability p can be obtained from (as discussed in Appendix for detail)

$$
\begin{aligned}
p &= \frac{2l}{\pi d} + \frac{2lK}{3\pi d}\cos 2\alpha + \frac{w}{d}, && l \leqslant d - r \\
&= \frac{2l}{\pi d} + \frac{2lK}{3\pi d}\cos 2\alpha + \frac{w}{d} - \frac{G(a_2, -a_2)}{6d(r-w)^2}, && d - r \leqslant l \leqslant d - w \\
&= \frac{l}{d}\left[E\left(\frac{\pi}{2}, a_3\right) + E\left(-a_3, -\frac{\pi}{2}\right)\right] + \frac{w}{d}\left[F\left(\frac{\pi}{2}, a_3\right) + F\left(-a_3, -\frac{\pi}{2}\right)\right] \\
&\quad - \frac{G(a_2, a_3) + G(-a_3, -a_2)}{6d(r-w)^2} + \left[1 - \frac{4}{3d}(r-w) - \frac{(r-d)^2}{d(r-w)} + \frac{2(r-d)}{d}\right] \\
&\quad \cdot F(a_3, -a_3) + \frac{2l}{d}\left(1 - \frac{r-d}{r-w}\right)E(a_3, -a_3) \\
&\quad - \frac{l^2}{d(r-w)}C(a_3, -a_3) + \frac{G(a_3, -a_3)}{6d(r-w)^2}, && d - w \leqslant l \leqslant d + r - 2w \\
&= \frac{l}{d}\left[E\left(\frac{\pi}{2}, a_3\right) + E\left(-a_3, -\frac{\pi}{2}\right)\right] + \frac{w}{d}\left[F\left(\frac{\pi}{2}, a_3\right) + F\left(-a_3, -\frac{\pi}{2}\right)\right] \\
&\quad - \frac{G(a_2, a_3) + G(-a_3, -a_2)}{6d(r-w)^2} + \left[1 - \frac{4}{3d}(r-w) - \frac{(r-d)^2}{d(r-w)} + \frac{2(r-d)}{d}\right] \\
&\quad [F(a_3, a_4) + F(-a_4, -a_3)] + \frac{2l}{d}\left(1 - \frac{r-d}{r-w}\right)[E(a_3, a_4) + E(-a_4, -a_3)] \\
&\quad - \frac{l^2}{d(r-w)}[C(a_3, a_4) + C(-a_4, -a_3)] \\
&\quad + \frac{1}{6d(r-w)^2}[G(a_3, a_4) + G(-a_4, -a_3)] + F(a_4, -a_4), \\
& && l \geqslant d + r - 2w.
\end{aligned}
$$

where the functions G, D, C, E, and F are defined in eqs. (A10)-(A14), respectively.

PRACTICAL EXAMPLE

For several years, the Geological Survey of Canada has been conducting a program of experimental airborne γ-ray spectrometer surveys applied to the location and mapping of radioactive mineral resources. Surveys have also been conducted to locate sources of radioactive contamination (Grasty, Richardson, and Knight, 1977).

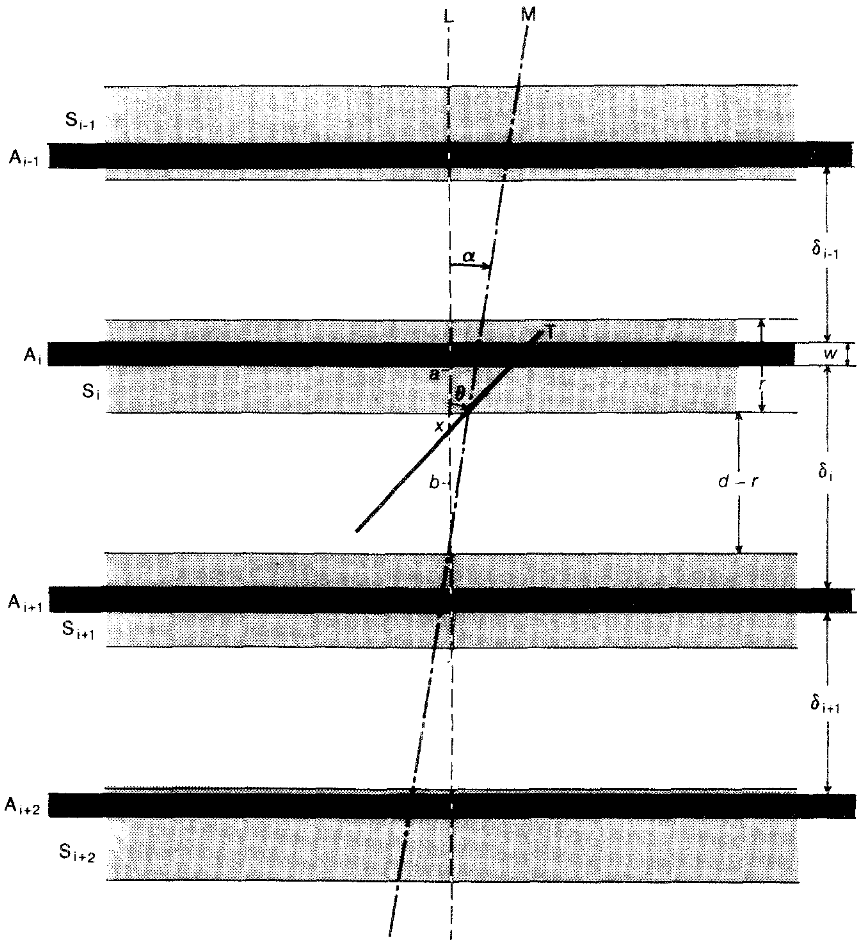

Fig. 6. x, θ, T, and L are the same as in Fig. 2. a, b, and S_is are the same as in Fig. 4 and M is the same as in Fig. 5. A grid of parallel strips A_is with breadth w is generated by choosing one strip A_i at random within each S_i and T is dropped on the grid so that θ has the density function in eq. (6). The probability that T intersects at least one of the strips is given in eq. (8).

Figure 1 is the flight path map for a survey flown in the Sharbot Lake Area of Eastern Ontario to investigate occurrences of uranium mineralization. The spacings between flight paths are approximately between 375 and 625 m and the breadth of the strips in this case might be considered to be about 100 m. Consequently, $d = 500$ m, $r = d/2$, and $w = d/5$ for this example. Let us consider two targets, T_1 and T_2, where T_1 has a preferred orientation $\alpha = 0.0$ and $K = 0.75$ and T_2 has $\alpha = 30.0$ and $K = 0.3$. As in eq. (6), K is a scale parameter and indicates density around α. For example, $K = 0.75$ for T_1 indicates that T_1

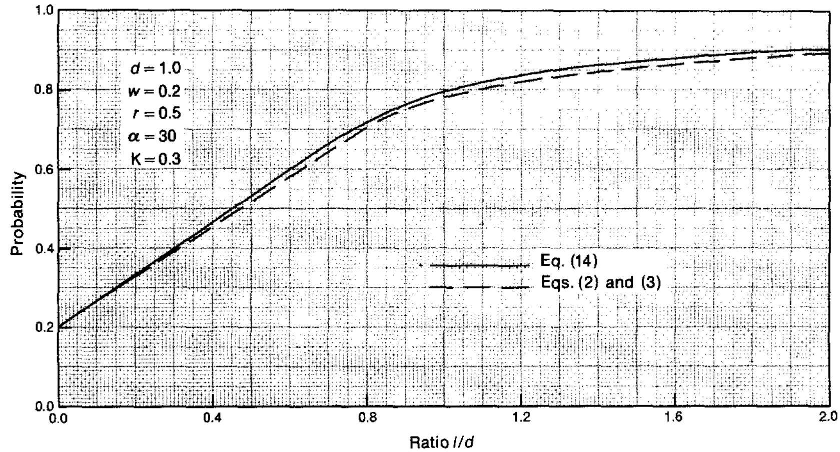

Fig. 7. Probability curve (solid line) using eq. (8) with respect to l/d when $r = 0.5d$ and $w = 0.2d$ for the target T_1. T_1 has a preferred orientation $\alpha = 0.0$, $K = 0.75$, and length l. Broken line using eqs. (2) and (3) is also shown for comparison. For example, suppose that the minimum length l of a target is desired with probability 0.5. We read the value of $l/d = 0.38$ (solid line), and thus the minimum length is 0.38 times the spacing d.

likely has an orientation near $\alpha = 0.0$. Using the given values for the parameters, p can be evaluated for various lengths l. Figs. 7 and 8 were constructed for the targets T_1 and T_2, respectively. The probabilities of intersections are shown with respect to the ratios between the lengths of the targets and the spacings of flight paths. From the figures, the spacing of flight paths can be determined for a given l and a probability of detection. Similarly, for a given spacing d and a

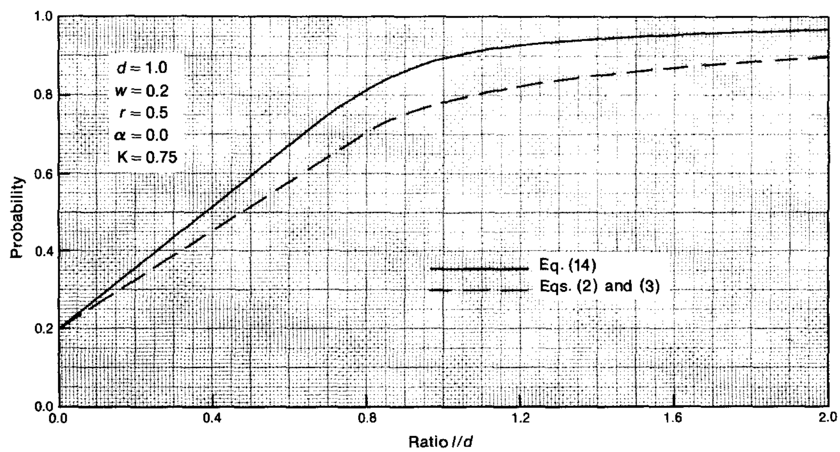

Fig. 8. Probability curve using eq. (8) with respect to l/d when $r = 0.5d$ and $w = 0.2d$ for the target T_2. T_2 has $\alpha = 30.0$ and $K = 0.3$.

given l, the probability of intersection can be evaluated. For example, for target T_1, results show 50% probability that this survey would locate a source of length 190 m or longer.

Figures 9-12 illustrate how the probability of interaction varies with the parameters r/d, w/d, α, and K, as given by eq. (8).

From Fig. 9, it is obvious that r exerts very little influence on the probability. On the other hand, as can be observed in Fig. 10, w has an effect on the probability for relatively short targets but not for longer ones. Figure 10 may also be used for studying efficiencies of search densities and survey instruments

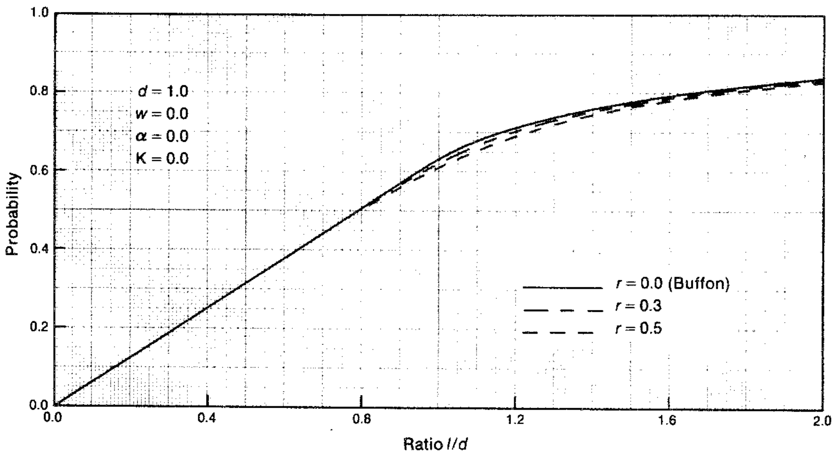

Fig. 9. Probability curves for r/d = 0.0, 0.3, and 0.5 where w/d = 0.0, α = 0.0, and K = 0.75.

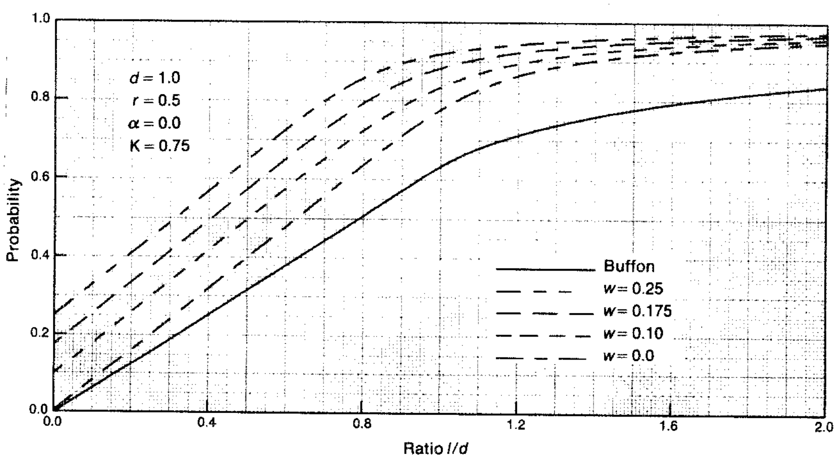

Fig. 10. Probability curves for w/d = 0.25, 0.175, 0.1, and 0.0 where r/d = 0.5, α = 0.0, and K = 0.75.

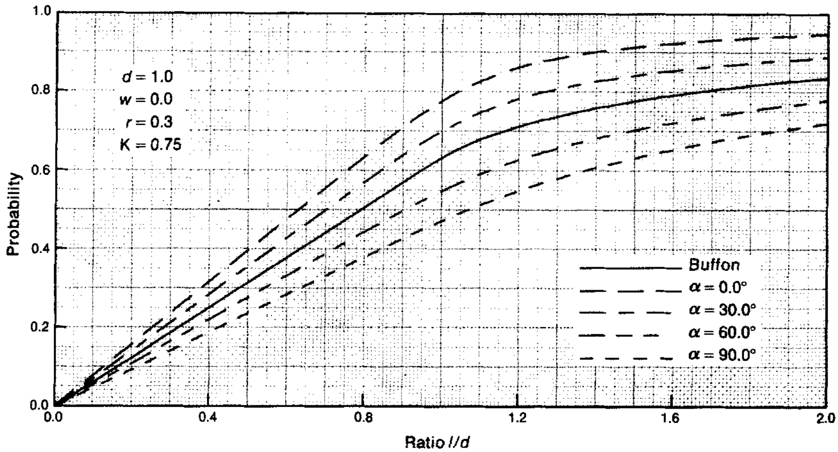

Fig. 11. Probability curves for $\alpha = 0.0, 30.0, 60.0$, and 90.0 where $r/d = 0.3$, $w/d = 0.0$, and $K = 0.75$.

(depending upon capabilities of detection through the breadths w of the strips) by comparing the resulting probabilities.

As expected, Fig. 11 confirms that the flight paths should be perpendicular to the most likely preferred orientation of the target ($\alpha = 0$ indicates the orientation is likely perpendicular to the flight paths; see Fig. 6). It is particularly important when K is close to 1.

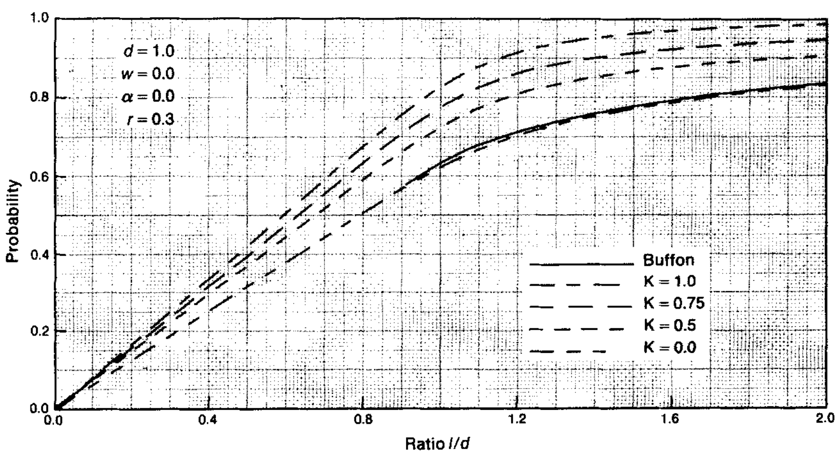

Fig. 12. Probability curves for $K = 1.0, 0.75, 0.5$, and 0.0 where $r/d = 0.3$, $w/d = 0.0$, and $\alpha = 0.0$.

CONCLUDING REMARKS

From this study, the following conclusions can be made

1. For a circular shaped target with diameter l, the probabilities of intersections are identical to the conditional probabilities $p_{1/\theta}, p_{2/\theta}, p_{3/\theta}, p_{4/\theta}$ and $p_{5/\theta}$ in eqs. (A2)-(A6), respectively. This is

$$
\begin{aligned}
p &= \frac{l}{d} + \frac{w}{d}, && l \leqslant d - r \\
&= \frac{l}{d} + \frac{w}{d} - \frac{(l+r-d)^3}{6d(r-w)^2}, && d - r \leqslant l \leqslant d - w \\
&= 1 + \frac{2}{d}(l+r-d) - \frac{4}{3d}(r-w) - \frac{(l+r-d)^2}{d(r-w)} + \frac{(l+r-d)^3}{6d(r-w)^2}, && \\
& && d - w \leqslant l \leqslant d + r - 2w \\
&= 1, && l \geqslant d + r - 2w
\end{aligned}
$$

2. For "short" or "long" targets, the probabilities in eq. (8) can be approximated by the p in eqs. (2) and (3), as can be seen in Figs. 9 to 12.
3. The probability in eq. (8) may be sufficiently accurate as an approximation of the probability for an elliptically shaped target when the major axis is about four times longer than the minor axis and the minor axis is relatively short.
4. However, as mentioned earlier, the geometric shape of the target in practice may be much more complex than the simple segment. Furthermore, the actual detection range is not the simple strip assumed. Much work is still needed to investigate the effect of removing some of the simplifying restrictions imposed in this study.

A computer program was written to compute p in eq. (8) for given l/d, r/d, w/d, α, and K. The program can be obtained on request from the author.

APPENDIX

In order to calculate the probability that needle T of length l intersects at least one of the strips of the grid characterized by the parameters w, r, and d

with $w \leqslant \frac{1}{2}r \leqslant \frac{1}{4}d$, as shown in Fig. 6, let

$$a_1 = \begin{cases} \cos^{-1}\left(\frac{r-2w}{l}\right), & l \geqslant r-2w \\ 0, & l < r-2w \end{cases}$$

$$a_2 = \begin{cases} \cos^{-1}\left(\frac{d-r}{l}\right), & l \geqslant d-r \\ 0, & l < d-r \end{cases}$$

$$a_3 = \begin{cases} \cos^{-1}\left(\frac{d-w}{l}\right), & l \geqslant d-w \\ 0, & l < d-w \end{cases}$$

$$a_4 = \begin{cases} \cos^{-1}\left(\frac{d+r-2w}{l}\right), & l \geqslant d+r-2w \\ 0, & l < d+r-2w \end{cases} \qquad \text{(A1)}$$

Then $0 \leqslant a_4 \leqslant a_3 \leqslant a_2 \leqslant a_1 \leqslant \pi/2$ because $w \leqslant \frac{1}{2}r \leqslant \frac{1}{4}d$. We may assume, without loss of generality, that the midpoint x of T takes a random point in $[0, \frac{1}{2}d]$, instead of $[a, b]$ shown in Fig. 6, because $b - a = \frac{1}{2}d$.

Let $p_{\cdot|\theta}$ be the conditional probability that T with a fixed orientation θ intersects a strip of the grid and let $p_{\cdot|\theta,x}$ be the probability that a fixed T (not only θ but also x of T are fixed) intersects the strips. These conditional probabilities depend upon the length l, where θ lies between $-\frac{1}{2}\pi$ and $\frac{1}{2}\pi$ and also where x lies in $[0, \frac{1}{2}d]$.

Case (1): $a_1 \leqslant \theta \leqslant \frac{1}{2}\pi$ or $-\frac{1}{2}\pi \leqslant \theta \leqslant -a_1$. If $l \leqslant r - 2w$, this case covers all θ, since $a_1 = a_2 = a_3 = a_4 = 0$. Otherwise, $a_1 > 0$ and it only covers T with θ in $[a_1, \frac{1}{2}\pi]$ or $[-\frac{1}{2}\pi, -a_1]$ where a_1 is defined in (A1). The conditional probability $p_{1|\theta,x}$ for a fixed x and θ is given by

$$\begin{aligned} p_{1|\theta,x} &= \frac{l\cos\theta + w}{r - w}, & x &\in [0, x_1] \\ &= \frac{x_2 - x}{r - w}, & x &\in [x_1, x_2] \\ &= 0, & x &\in [x_2, d/2] \end{aligned}$$

where $x_1 = \frac{1}{2}r - \frac{1}{2}l\cos\theta - w$ and $x_2 = \frac{1}{2}r + \frac{1}{2}l\cos\theta$. Thus, $p_{1|\theta}$ for the given θ with $a_1 \leqslant \theta \leqslant \frac{1}{2}\pi$ or $-\frac{1}{2}\pi \leqslant \theta \leqslant -a_1$ is obtained from

$$p_{1|\theta} = \frac{2}{d}\int_0^{x_1} \frac{l\cos\theta + w}{r - w}\,dx + \frac{2}{d}\int_{x_1}^{x_2} \frac{x_2 - x}{r - w}\,dx$$

$$= \frac{1}{d}(l\cos\theta + w) \tag{A2}$$

This conditional probability $p_{1|\theta}$ will be used to calculate the probability p of intersection.

Case (2):

$$a_2 \leqslant \theta \leqslant a_1 \quad \text{or} \quad -a_1 \leqslant \theta \leqslant -a_2; \qquad l > r - 2w.$$

This case only occurs when $l > r - 2w$, the $p_{2|\theta,x}$ for a fixed x and θ with $a_2 \leqslant \theta \leqslant a_1$ or $-a_1 \leqslant \theta \leqslant -a_2$ is given by

$$\begin{aligned} p_{2|\theta,x} &= 1, && x \in [0, x_3] \\ &= \frac{x_2 - x}{r - w}, && x \in [x_3, x_2] \\ &= 0, && x \in [x_2, d/2] \end{aligned}$$

where $x_3 = \frac{1}{2}l\cos\theta + w - \frac{1}{2}r$. Thus,

$$p_{2|\theta} = \frac{2}{d}\int_0^{x_3} dx + \frac{2}{d}\int_{x_3}^{x_2} \frac{x_2 - x}{r - w}\,dx$$

$$= \frac{1}{d}(l\cos\theta + w) \tag{A3}$$

Case (3):

$$a_3 < \theta \leqslant a_2 \quad \text{or} \quad -a_2 \leqslant \theta < -a_3; \qquad l > d - r$$

$$\begin{aligned} p_{3|\theta,x} &= 1, && x \in [0, x_3] \\ &= \frac{x_2 - x}{r - w}, && x \in [x_3, x_4] \\ &= \frac{x_2 - x_4}{r - w} - \frac{(x_2 - x)(x - x_4)}{(r - w)^2}, && x \in [x_4, d/2] \end{aligned}$$

where $x_4 = d - \frac{1}{2} l \cos\theta - \frac{1}{2} r$. Thus

$$p_{3|\theta} = \frac{2}{d}\left[\int_0^{x_3} dx + \int_{x_3}^{x_4} \frac{x_2 - x}{r - w}\, dx + \int_{x_4}^{d/2} \left(\frac{x_2 - x_4}{r - w} - \frac{(x_2 - x)(x - x_4)}{(r - w)^2}\right) dx\right]$$

$$= \frac{1}{d}(l\cos\theta + w) - \frac{(l\cos\theta + r - d)^3}{6d(r - w)^2} \tag{A4}$$

Case (4):

$$a_4 < \theta \leqslant a_3 \text{ or } -a_3 \leqslant \theta < -a_4; \qquad l > d - w$$

$$p_{4|\theta,x} = 1, \qquad x \in [0, x_3]$$

$$= \frac{x_2 - x_4}{r - w} - \frac{(x_2 - x)(x - x_4)}{(r - w)^2}, \qquad x \in [x_3, d/2]$$

Thus,

$$p_{4|\theta} = \frac{2}{d}\int_0^{x_3} dx + \frac{2}{d}\int_{x_3}^{d/2} \frac{x_2 - x_4}{r - w} - \frac{(x_2 - x)(x - x_4)}{(r - w)^2}\, dx$$

$$= 1 + \frac{2}{d}(l\cos\theta + r - d) - \frac{4}{3d}(r - w) - \frac{(l\cos\theta + r - d)^2}{d(r - w)} + \frac{(l\cos\theta + r - d)^3}{6d(r - w)^2} \tag{A5}$$

Case (5):

$$-a_4 \leqslant \theta \leqslant a_4; \qquad l > d + r - 2w$$

$$p_{5|\theta,x} = 1 \qquad \text{for all} \quad x \in [0, d/2]$$

Thus,

$$p_{5|\theta} = 1 \tag{A6}$$

Therefore, the probability p of intersection is obtained from

$$p = \int_{-\pi/2}^{-a_1} p_{1|\theta} f(\theta)\, d\theta + \int_{-a_1}^{-a_2} p_{2|\theta} f(\theta)\, d\theta + \int_{-a_2}^{-a_3} p_{3|\theta} f(\theta)\, d\theta$$

$$+ \int_{-a_3}^{-a_4} p_{4|\theta} f(\theta)\, d\theta + \int_{-a_4}^{a_4} p_{5|\theta} f(\theta)\, d\theta + \int_{a_4}^{a_3} p_{4|\theta} f(\theta)\, d\theta$$

$$+ \int_{a_3}^{a_2} p_{3|\theta} f(\theta)\, d\theta + \int_{a_2}^{a_1} p_{2|\theta} f(\theta)\, d\theta + \int_{a_1}^{\pi/2} p_{1|\theta} f(\theta)\, d\theta \qquad \text{(A7)}$$

However, eq. (A7) can be separately solved depending upon the length l.

(a) $l < d - r$.

Since $a_2 = a_3 = a_4 = 0$ in eq. (A1) and $p_{1|\theta} = p_{2|\theta}$, p in (A7) becomes

$$p = \int_{-\pi/2}^{\pi/2} \frac{1}{d} (l \cos\theta + w) \frac{1}{\pi} (1 + K \cos 2(\alpha - \theta))\, d\theta$$

$$= \frac{2l}{\pi d} + \frac{2lK}{3\pi d} \cos 2\alpha + \frac{w}{d} \qquad \text{(A8)}$$

(b) $d - r \leqslant l < d - w$.

Since $a_3 = a_4 = 0$, by substituting equations in (A2), (A3) and (A4) into (A7), p becomes

$$p = \int_{-\pi/2}^{\pi/2} \frac{1}{d} (l \cos\theta + w) \frac{1}{\pi} (1 + K \cos 2(\alpha - \theta))\, d\theta$$

$$- \int_{-a_2}^{a_2} \frac{(l \cos\theta + r - d)^3}{6d(r - w)^2} \frac{1}{\pi} (1 + K \cos 2(\alpha - \theta))\, d\theta$$

$$= \frac{2l}{\pi d} + \frac{2lK}{3\pi d} \cos 2\alpha + \frac{w}{d} - \frac{G(a_2, -a_2)}{6d(r - w)^2} \qquad \text{(A9)}$$

where

$$G(a, b) = \int_b^a (l \cos\theta + r - d)^3 \frac{1}{\pi} [1 + K \cos 2(\alpha - \theta)]\, d\theta$$

$$= l^3 D(a, b) + 3l^2 (r - d) [(a, b) + 3l(r - d)^2 E(a, b)] + (r - d)^3 F(a, b), \qquad \text{(A10)}$$

$$D(a, b) = \int_b^a \cos^3 \theta \, \frac{1}{\pi} \, [1 + K \cos 2(\alpha - \theta)] \, d\theta$$

$$= \left(\sin a - \frac{1}{3} \sin^3 a - \sin b + \frac{1}{3} \sin^3 b\right) \left(\frac{1}{\pi} + \frac{3K}{5\pi} \cos 2\alpha\right)$$

$$+ \frac{2K}{5\pi} \cos 2\alpha(\sin a \cos^4 a - \sin b \cos^4 b)$$

$$- \frac{2K}{5\pi} \sin 2\alpha(\cos^5 a - \cos^5 b), \tag{A11}$$

$$C(a, b) = \int_b^a \cos^2 \theta \, \frac{1}{\pi} \, (1 + K \cos 2(\alpha - \theta)) \, d\theta$$

$$= (2a + \sin 2a - 2b - \sin 2b) \left(\frac{1}{\pi} + \frac{K}{4\pi} \cos 2\alpha\right)$$

$$- \frac{K}{4\pi} \cos 2\alpha \left(a - \frac{1}{4} \sin 4a - b + \frac{1}{4} \sin 4b\right)$$

$$- \frac{K}{2\pi} \sin 2\alpha(\cos^4 a - \cos^4 b), \tag{A12}$$

$$E(a, b) = \int_b^a \cos \theta \, \frac{1}{\pi} \, [1 + K \cos 2(\alpha - \theta)] \, d\theta$$

$$= (\sin a - \sin b) \left(\frac{1}{\pi} + \frac{K}{\pi} \cos 2\alpha\right)$$

$$- \frac{2K}{3\pi} [\cos 2\alpha(\sin^3 a - \sin^3 b) + \sin 2\alpha(\cos^3 a - \cos^3 b)], \tag{A13}$$

$$F(a, b) = \int_b^a \frac{1}{\pi} \, [1 + K \cos 2(\alpha - \theta)] \, d\theta$$

$$= \frac{1}{\pi} (a - b) + \frac{K}{2\pi} [\cos 2\alpha(\sin 2a - \sin 2b) - \sin 2\alpha(\cos 2a - \cos 2b)]. \tag{A14}$$

(c) $d - w \leqslant l < d + r - 2w$.

Similarly, by substituting equations in (A2), (A3), (A4), and (A5) into (A7), p becomes

$$p = \int_{a_2}^{\pi/2} \frac{1}{d} (l \cos\theta + w) f(\theta)\, d\theta + \int_{-\pi/2}^{-a_2} \frac{1}{d} (l \cos\theta + w) f(\theta)\, d\theta$$

$$+ \int_{a_3}^{a_2} p_{3/\theta} f(\theta)\, d\theta + \int_{-a_2}^{-a_3} p_{3/\theta} f(\theta)\, d\theta + \int_{-a_3}^{a_3} p_{4/\theta} f(\theta)\, d\theta$$

$$= \frac{l}{d}\left[E\left(\frac{\pi}{2}, a_3\right) + E\left(-a_3, \frac{\pi}{2}\right)\right] + \frac{w}{d}\left[F\left(\frac{\pi}{2}, a_3\right) + F\left(-a_3, -\frac{\pi}{2}\right)\right]$$

$$- \frac{G(a_2, a_3) + G(-a_3, -a_2)}{6d(r-w)^2} + \left[1 - \frac{4}{3d}(r-w) - \frac{(r-d)^2}{d(r-w)} + \frac{2(r-d)}{d}\right]$$

$$\cdot F(a_3, -a_3) + \frac{2l}{d}\left(1 - \frac{r-d}{r-w}\right) E(a_3, -a_3) - \frac{l^2}{d(r-w)} C(a_3, -a_3)$$

$$+ \frac{G(a_3, -a_3)}{6d(r-w)^2}. \tag{A15}$$

(d) $l \geqslant d + r - 2w$.

By substituting (A2), (A3), (A4), (A5), and (A6) into (A7), p becomes

$$p = \int_{a_2}^{\pi/2} \frac{1}{d} (l \cos\theta + w) f(\theta)\, d\theta + \int_{-\pi/2}^{-a_2} \frac{1}{d} (l \cos\theta + w) f(\theta)\, d\theta$$

$$+ \int_{a_3}^{a_2} p_{3/\theta} f(\theta)\, d\theta + \int_{-a_2}^{-a_3} p_{3/\theta} f(\theta)\, d\theta + \int_{a_4}^{a_3} p_{4/\theta} f(\theta)\, d\theta$$

$$+ \int_{-a_3}^{-a_4} p_{4/\theta} f(\theta)\, d\theta + \int_{-a_3}^{a_4} f(\theta)\, d\theta$$

$$= \frac{l}{d}\left[E\left(\frac{\pi}{2}, a_3\right) + E\left(-a_3, -\frac{\pi}{2}\right)\right] + \frac{w}{d}\left[F\left(\frac{\pi}{2}, a_3\right) + F\left(-a_3, -\frac{\pi}{2}\right)\right]$$

$$- \frac{G(a_2, a_3) + G(-a_3, -a_2)}{6d(r-w)^2} + \left[1 - \frac{4}{3d}(r-w) - \frac{(r-d)^2}{d(r-w)} + \frac{2(r-d)}{d}\right]$$

$$\cdot [F(a_3, a_4) + F(-a_4, -a_3)] + \frac{2l}{d}\left(1 - \frac{r-d}{r-w}\right) [E(a_3, a_4) + E(-a_4, -a_3)]$$

$$- \frac{l^2}{d(r-w)} [C(a_3, a_4) + C(-a_4, -a_3)] + \frac{1}{6d(r-w)^2}$$

$$\cdot [G(a_3, a_4) + G(-a_4, -a_3)] + F(a_4, -a_4) \tag{A16}$$

ACKNOWLEDGMENTS

I am indebted to Dr. K. A. Richardson and Mr. J. Carson of Geological Survey of Canada for their valuable comments on an earlier draft of this manuscript.

REFERENCES

Agos, W. G., 1955, Line spacing effect and determination of optimum spacing illustrated by Marmora, Ontario magnetic anomaly: Geophysics, v. 20, no. 4, p. 871-885.

Grasty, R. L., Richardson, K. A., and Knight, G. B., 1977, Airborne detection of small radioactive sources, *in* Aerial techniques for environmental monitoring: Amer. Nuclear Soc., Nevada, p. 182-192.

Grasty, R. L., Kosanke, K. L., and Foote, R. S., 1979, Fields of view of airborne gamma-ray detectors: Geophysics, v. 44, no. 8, p. 1447-1457.

Johnson, N. I. and Kotz, S., 1970, Continuous univariate distributions 2: Houghton Mifflin, Boston, Mass., 306 p.

Kendall, M. G. and Moran, P. A. P., 1963, Geometrical probability: Griffin, London, 125 p.

Marriot, F. H. C., 1969, Associated directions: Biometrics, v. 25, no. 4, p. 775-776.

Marriot, F. H. C., 1971, Buffon's problems for non-random distribution: Biometrics, v. 27, no. 1, p. 233-235.

McCammon, R. B., 1977, Target intersection probabilities for parallel-line and continuous grid types of search: Math. Geol., v. 9, no. 4, p. 369-382.

Santalo, L. A., 1976, Integral geometry and geometric probability: Addison-Wesley, Mass., 404 p.

Solomon, H., 1978, Geometric probability: Soc. Indust. Appl. Math., Penn., 175 p.

Watson, G. S., 1978, Characteristic statistical problems of stochastic geometry, *in* R. E. Miles and J. Serra, (eds.), Geometrical probability and biological structures: Buffon's 200th Anniversary: Springer-Verlag, N.Y., p. 215-233.